Sedimentation of short-lived fluid-solid suspensions

Laurence Girolami, Frédéric Risso, Ahmad Amin, Loïc Rousseau, Andrea Bondesan, Stéphane Bonelli

▶ **To cite this version:**

Laurence Girolami, Frédéric Risso, Ahmad Amin, Loïc Rousseau, Andrea Bondesan, et al.. Sedimentation of short-lived fluid-solid suspensions. Physics of Fluids, 2024, 36 (11), 10.1063/5.0231788 . hal-04736158v1

HAL Id: hal-04736158

https://hal.science/hal-04736158v1

Submitted on 14 Oct 2024 (v1), last revised 27 Nov 2024 (v2)

HAL is a multi-disciplinary open access archive for the deposit and dissemination of scientific research documents, whether they are published or not. The documents may come from teaching and research institutions in France or abroad, or from public or private research centers.

L'archive ouverte pluridisciplinaire **HAL**, est destinée au dépôt et à la diffusion de documents scientifiques de niveau recherche, publiés ou non, émanant des établissements d'enseignement et de recherche français ou étrangers, des laboratoires publics ou privés.

Sedimentation of short-lived fluid-solid suspensions

Laurence Girolami,[1, 2, a)] Frédéric Risso,[3] Ahmad Amin,[1] Loïc Rousseau,[1] Andrea Bondesan,[4] and Stéphane Bonelli[2]

[1)]*GéHCO, Université de Tours, Campus Grandmont, 37200 Tours, France.*

[2)]*RECOVER, INRAE−Aix-Marseille Université, 13100 Aix-en-Provence, France.*

[3)]*IMFT, CNRS−Université de Toulouse, 31400 Toulouse, France.*

[4)]*Dipartimento di Scienze Matematiche, Fisiche e Informatiche, Università di Parma, Parma, Italy.*

(Dated: 5 October 2024)

In this study, we propose a particle sedimentation/aggradation law for homogeneous concentrated suspensions. This law, valid in the Stokes flow regime, can be used to describe the sedimentation process observed in short-lived rapid flows, developed at high Reynolds number, that can be described as low-viscosity quasi-parallel flows traveling at constant velocity and that progressively sediment during the dominant phase of transport to leave a triangular or trapezoidal deposit of constant slope. The particle aggradation velocity can thus be predicted from the product of the mean flow velocity and the deposit slope and turns out to be roughly similar to that measured from static suspensions of same concentration, provided that the flow Reynolds number, based on the mean flow velocity, the fluid properties and the particles size remains inferior to a few hundred, such as the mixture agitation can not disturb the sedimentation process. These important results provide the possibility of describing the depositional dynamics during the final stage of extreme events, as well as to infer the mixture rheology, from physical parameters that can be easily measured in the field.

[a)]Electronic mail: laurence.girolami@univ-tours.fr

I. INTRODUCTION

Some examples of natural particulate suspensions, such as pyroclastic flows, lahars or non colloidal mud-flows, involve different types of sediments and fluids for a wide range of particle concentrations. These devastating phenomena, usually formed during extreme events, are short-lived and difficult to observe[1–3]. Their deposits are therefore usually carefully studied in the aim of inferring information on the flow dynamics[4–8]. Simplified laboratory experiments can provide guides for describing these complex geophysical mass flows and help to predict their runout and deposits geometry[9–11]. In this study, we focus on sediment-laden flows, characterized by a high concentration of particles, whose size and density are large enough (greater than a few tens of microns and denser than the surrounding fluid) to be considered as non-colloidal and non-cohesive (*i.e.* no attraction, adhesion, or capillary forces exist between particles) which travel under the action of gravity. In nature, basal pyroclastic flows are made with hot volcanic ash suspended into a gas raised at temperatures close to 500^oC which makes particles non cohesive[12], while lahars commonly involve coarser volcanic tephras or fluvial sediments suspended into water raised at temperatures close to 80^oC[13]. Once these conditions filled, mixtures can be described in a simplified way, by considering almost homogeneous (fully fluidized) suspensions[4,11,14], with no significant gradients of concentration[15], from which observations and quantitative measurements can be performed[16]. Most of recent investigations devoted to geophysical mass flows focused on the two extreme cases where a highly concentrated mixture, slightly expanded (close to the packing state), is dominated by the excess of pore pressure[17–19]; or a dilute turbulent surge dominated by vorticity and agitation[20–22]. Otherwise, further important scientific issues concern the internal flow stratification that leads to the formation of a basal concentrated underflow and an upper dilute current between which interactions or detachment processes can occur during propagation[23–26]. However, no preliminary study has been proposed to describe and predict the sedimentation velocity in particle-laden flows, as well as the geometry of the final deposit. In this paper, we aim at investigating how the suspension flows in cases where the concentrated mixture is not underwent to segregation in size or density[27–30] but is sufficiently expanded to be considered as homogeneous, then exploring and describing how it sediments[15]. In doing so, the mixture can be described as an equivalent fluid of known physical properties in which dense and large particles are falling by gravity. The flow runout is then governed by the separation between the two phases so that the suspension is at rest when all particles have settled and the fluid is mostly expelled from the deposit.

This amounts at exploring the stopping phase of natural flows, when traveling far from the source down gentle slopes and dominated by sedimentation[6,28]. These depositional processes however develop at a much slower velocity than that of the flow, such as being described independently[16,31], and thus requiring both the description of the sedimentation process as well as that of the flow in relevant controled experiments. In a first part, depositional aspects are investigated using fluidization techniques which make possible the reproduction of homogeneous fully fluidized suspensions (*i.e.* when the mixture is sufficiently expanded, greater than 10% in volume[32]), in which the mixture density and particle concentration can be carefully inferred. Defluidization experiments (also termed *bed collapse tests*[33,34]) are performed to reliably measure the settling velocity of the bed surface as well as the aggradation velocity of the deposit at different concentrations, when the particles motion is mainly vertical and the mixture is not traveling. Once explored, we can then reasonably wonder whether this measured velocity is valid for short-lived suspension flows dominated by sedimentation. In a second part, dam-break flows of well-calibrated mixtures of different concentrations are generated by releasing suspensions down a flat bottom to explore their kinematics and deposition dynamics. From these rapid flows, the mean velocity, runouts, and deposit features can be simply measured, while the aggradation velocity of the basal deposit at different times and spaces requires additional visualization techniques. In this paper, we present results obtained for fluid-solid suspensions, made with different particles and fluids, using this experimental approach and derive generic laws that can be used in practice to infer the sedimentation dynamics in natural flows from measurable parameters.

II. SEDIMENTATION OF STATIC SUSPENSIONS

A. Presentation of experiments

The principle of the experiments consists in first fluidizing uniformly a heap of particles, of solid volume fraction Φ_{pack}, by injecting a fluid at the base of a reservoir until obtaining a homogeneous and stable suspension (Figure 1). The relevance of reproducing a particulate suspension in this way lies in the ability of controling the mixture properties (namely the solid volume fraction Φ_s and the mixture density $\rho_m = \Phi_s\rho_s + (1-\Phi_s)\rho_f$ through the mixture expansion rate, defined as the ratio between the fluidized suspension thickness h_s and the initial particle bed thickness h_d, such as : $\frac{h_s}{h_d} = \frac{\Phi_{pack}}{\Phi_s}$ (Figure 1). Once fluidized, the drag force balances the weight of parti-

cles, then suspended into the surrounding fluid, such as the pressure drop across the bed becomes independent of the superficial fluid velocity U_f and the mixture starts expanding uniformly at a rate proportional to U_f[35,36]. From a threshold expansion rate, controled by the Stokes number determined for the fluid-particle system $St_0 = \frac{g(\rho_s+\frac{1}{2}\rho_f)(\rho_s-\rho_f)d^3}{18\ \mu_f^2}$, the mixture becomes unstable and heterogeneous (including concentration gradients)[15]. The sedimentation of particles is then investigated from the settling of the suspension surface, by cutting the fluid supply. Since the ratio between the mean particle diameter and the reservoir dimensions remains very small in experiments ($< 5.10^{-4}$), boundary effects were considered as negligible, so that the velocity U_{sed} at which particles move through a static fluid at a given solid volume fraction Φ_s is expected identical to the fluidizing velocity U_f at which the fluid moves through static particles by a Galilean transformation[37].

The singularity of these experiments lies in the choice of the fluid-particle systems involved in the suspensions. In this study, the mean particle diameter d varied by a factor 5 from the finest material to the coarsest one; the solid density ρ_s varied by a factor 2 from the lightest material to the denser one; while the particle shape varied from spherical to angular. Two different types of fluids (gas and liquid) were employed and allowed to vary the fluid density ρ_f over 3 orders of magnitude; and its viscosity μ_f over 2 orders of magnitude. The physical properties of the materials, fluids, and suspensions are summarized in Table I). The choice of investigating such fluid-solid suspensions was motivated by getting fully fluidized suspensions capable of approaching the natural conditions, but also of being described as homogeneous mixtures[15,32], which implies specific technical constraints.

Gas-solid suspensions were made with fine synthetical or natural powders, ranged from 65 μm to 80 μm, with hot air (180^oC). Such particles ($St_0 = \mathscr{O}(10^3)$) turn out to be much finer and lighter than those commonly employed in fluidized beds for engineering and industrial applications. They can fluidize and expand significantly (until 50 vol%) when the system is heated at a temperature sufficiently high ($\geq 150^oC$) to reduce cohesive forces attributed to the air moisture[11,16,34]. Liquid-solid suspensions were made with synthetical particles, ranged from 160 μm to 335 μm, at room temperature ranged between 15^oC and 35^oC. For those materials ($St_0 = \mathscr{O}(10^1)$), the particulate regime of fluidization is associated with a uniform expansion up to 350 vol%, but requires a well-calibrated porous medium located beneath the fluidization rig and a closed-loop operation system[15]. Once these conditions obtained, collapse experiments of homogenous suspensions allow to investigate the deposition processes in static or flowing suspensions of different solid volume

fraction.

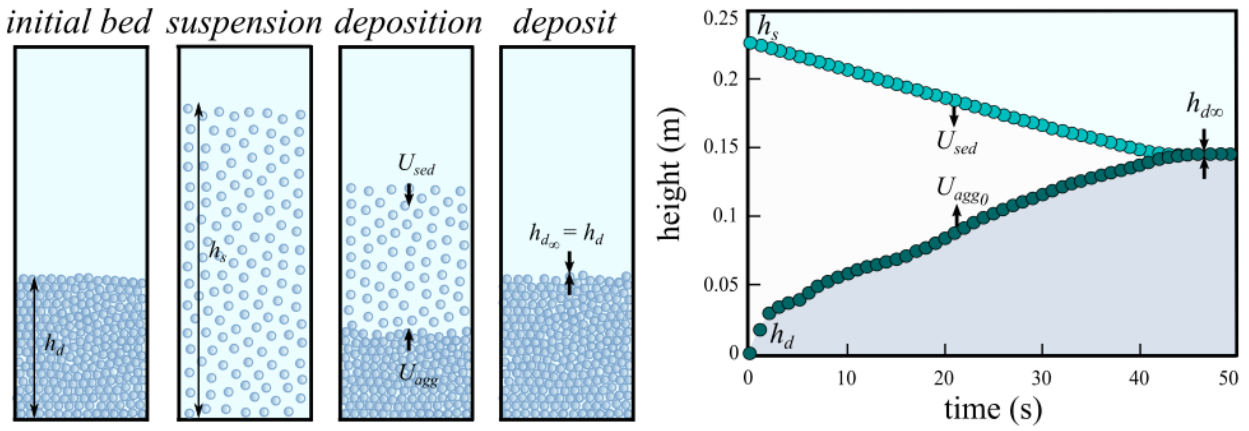

FIG. 1. On the left : mixture stratification by sedimentation. During fluidization, the suspension is homogeneous and characterized by a concentration Φ_s. After cutting the fluid supply, the suspension settles at a speed U_{sed} by expelling a layer of fluid at the top and forming a deposit that thickens from the base at a speed U_{agg_0}. At the end of the experiment, the upper and lower interfaces collapse when the phase separation is completed. The kinematics of each interface depends on the initial mixture concentration. On the right : suspension height h_s and deposit height h_d as a function of time during sedimentation of GB^1 for $\Phi_s = 0.415$.

Measurements in static suspensions of both the suspension thickness h_s and the deposit height h_d with time was performed at a given Φ_s and point that instantaneous velocities U_{sed} and U_{agg_0} remain approximately constant with time (Figure 1), while their mean values can be expressed from each other through the mass conservation, under the assumption of a constant Φ_s with time and space, such as :

$$U_{agg_0} = \frac{U_{sed}}{\left(\frac{\Phi_{pack}}{\Phi_s} - 1\right)}. \tag{1}$$

Thus, mean values of U_{agg_0} can be deduced from simple measurements of U_{sed} in homogeneous suspensions.

B. Dimensional analysis

The description of the sedimentation process of particulate suspensions involves 7 independent physical parameters, listed as follows : the mean particle diameter d, the effective density includ-

ing the mass of fluid displaced by a spherical particle $\rho_s + \frac{1}{2}\rho_f$, the reduced weight of particles $g(\rho_s - \rho_f)$, the fluid density ρ_f, the fluid viscosity μ_f, the solid volume fraction of the suspension Φ_s, the solid volume fraction of the initial particle bed or deposit Φ_{pack}, which involves three dimensions and leads to build $7-3=4$ non-dimensional groups, defined hereafter.

(1) The solid volume fraction of the suspension $\Phi_s = \frac{M_p/\rho_s}{V_s}$, that describes the particle concentration of the mixture;

(2) the solid volume fraction normalized by its value at packing $\frac{\Phi_s}{\Phi_{pack}}$ (which corresponds to the inverse of the expansion rate $\frac{h_s}{h_d}$) that characterizes the microstructure of the interstices within the suspension and ranges from 0 to 1;

(3) the Reynolds number, $Re = \frac{\rho_f d U_{sed}}{\mu_f}$, based on the sedimentation velocity and the particles diameter, that accounts for the role of the fluid inertia relatively to viscous stresses;

(4) the Stokes number, $St = \frac{(\rho_s + \frac{1}{2}\rho_f) d U_{sed}}{\mu_f}$, that characterizes the particle inertia relatively to the fluid viscosity.

The description of the sedimentation process in particulate suspensions depends on Φ_s, $\frac{\Phi_s}{\Phi_{pack}}$, Re, St. According to the type of solid particles and fluid involved in the mixture, Re and St can be neglected. In cases of suspensions made with fine (of a few tens/hundreds of micrometers), non cohesive particles mixed with gas or liquid, the Reynolds number remains low so that the fluid inertia has no effect on the sedimentation velocity and can be discarded from the analysis. When suspended particles are coarser (of millimeter size), Re becomes high enough to consider that the fluid inertia can significantly disturb U_{sed} and has to be accounted for in the sedimentation law. Otherwise, in cases of suspensions made with light particles (characterized by a small density ratio between the solid and the fluid $\frac{\rho_s}{\rho_f} \ll 1$), the Stokes number remains low enough to be discarded from the analysis. When suspended particles are heavy ($\frac{\rho_s}{\rho_f} \gg 1$), the Stokes number becomes high so that the effect of the particle inertia impacts the sedimentation velocity and has to be taken into account in the general law, which is however missing from the classical fluidization/sedimentation laws of the literature[38–40]. In these experiments, Re ranged from 8.10^{-3} to 2.5, with most of the values less than 0.5, and remains very low compared to St, ranged from 0.2 to 50, with most of the values greater than 5. The effect of the fluid inertia is thus negligible in this study contrary to that of the particles, as in geophysical mass flows (*i.e.* pyroclastic flows or lahars) in which sedimentation of volcanic ash, lapillis, or fine sands develops at low Re but variable St (with higher values in pyroclastic flows).

This allows to discard Re from the description of this process in the follow of this study.

Physical parameters	GB^1-W	GB^2-W	GB^3-W	Ash^1-A	Ash^2-A	$FCC-A$
Particles diameter d [μm]	160	240	335	80	65	70
Solid density ρ_s [kg.m^{-3}]	2500	2500	2500	1600	1490	1420
Fluid density ρ_f [kg.m^{-3}]	10^3	10^3	10^3	0.80	0.80	0.80
Fluid viscosity μ_f [Pa.s]	10^{-3}	10^{-3}	10^{-3}	10^{-5}	10^{-5}	10^{-5}
Mixture concentration Φ_s	0.16 - 0.96	0.37 - 0.96	0.54 - 0.96	0.70 - 0.94	0.71 - 0.95	0.82 - 0.95
Range of $\frac{\Phi_s}{\Phi_{pack}}$	0.16 - 0.96	0.37 - 0.96	0.54 - 0.96	0.70 - 0.94	0.71 - 0.95	0.82 - 0.95
St_0=$\frac{g(\rho_s-\rho_f)(\rho_s+\frac{1}{2}\rho_f)d^3}{18\ \mu_f^2}$	10	35	95	1200	550	650

TABLE I. Experimental parameters obtained with both liquid-solid suspensions made with glass beads (GB^1; GB^2; GB^3) and water (W) taken at 20^{o}C and gas-solid suspensions made with volcanic ash (Ash^1; Ash^2) or chemical catalysts (FCC) and air (A) both heated at 180^{o}C.

Based on the Stokes velocity $U_0 = \frac{g(\rho_s-\rho_f)d^2}{18\ \mu_f}$, the Stokes number writes $St_0 = \frac{g(\rho_s+\frac{1}{2}\rho_f)(\rho_s-\rho_f)d^3}{18\ \mu_f^2}$ and only depends on the properties of the material and fluid involved in the suspensions. Note that $St_0 = \left(\frac{\rho_s+\frac{1}{2}\rho_f}{\rho_f}\right) Ar$, where Ar, the Archimede number compares the inertia of gravity-induced motions to viscous forces. The description of the sedimentation process henceforth depends on the three non dimensional groups : Φ_s, $\frac{\Phi_s}{\Phi_{pack}}$, St_0.

C. The sedimentation law in the Stokes flow regime

Measurements of U_f and U_{sed} have been performed with an accuracy of $\pm 3\%$ for different fluid-solid suspensions presented in Table I and allow us to cover a wide range of mixture concentrations (from the packing state to the dilute one), assessed with an accuracy of $\pm 4\%$, in order to propose a sedimentation law that depends on the relevant non-dimensional groups (Φ_s, $\frac{\Phi_s}{\Phi_{pack}}$, St_0)[15]. This law, valid in the Stokes flow regime, represents an extension to the popular Richardson-Zaki approach[38], where U_{sed}, expressed by $U_{sed} = U_i(1-\Phi_s)^n$, depends on two independent parameters U_i and n. In their empirical formulae, U_i is a calibration parameter required to gather the data and does not correspond to the terminal fall velocity of an isolated particle U_0, but where discrepancy to this value $\frac{U_i}{U_0}$ depends on St_0, which is missing from their dimensional analysis[15]. The exponent n seems depending on the flow regime through the Reynolds number Re ($n = 4.65$ in the Stokes

flow regime), but more realistically needs to be adjusted from experimental data, taking $n = 3.75$ for the present measurements[15].

From experiments, the mean values of U_{sed} appear approximately equal to U_f, highlighting negligible wall effects and allow us to propose a simple model involving the relevant parameters St_0, Φ_{pack} and Φ_s, *i.e.* which respectively characterizes the fluid-particle system, the solid volume fraction of the granular pile and that of the suspension. Velocity U_{sed} is observed to decrease with $\frac{\Phi_s}{\Phi_{pack}}$ and St_0, *i.e.* when the effective viscosity of the mixture increases. Result analysis exposes that experimental data can be gathered on a master curve capable of predicting particles sedimentation velocities from static suspensions (equations (2), (3), (4); Figure 2). The sedimentation velocity of a suspension differs from the theoretical Stokes velocity U_0 of a single particle of negligible inertia ($St_0 = 0$) falling in a fluid at rest of high viscosity ($Re = 0$), because of the three following effects : (1) the mixture density affects the buoyancy force acting on each particle through a (1 - Φ_s) factor; (2) the fluid that flows through interstices opposes the particle motion and gives rise to a decreasing hindering function $F_1\left(\frac{\Phi_s}{\Phi_{pack}}\right)$; (3) the particles inertia increases the fluctuating velocity, then the drag force acting on each particle, leading to an additional hindering effect accounted by the decreasing function $F_2\left(St_0\right)$. Accurate predictions of U_{sed} are given by the following expressions :

$$U_{sed} = U_0\ (1-\Phi_s)\ F_1\left(\frac{\Phi_s}{\Phi_{pack}}\right) F_2\left(St_0\right) \tag{2}$$

$$F_1\left(\frac{\Phi_s}{\Phi_{pack}}\right) = \frac{1}{\exp\left(1.9\frac{\Phi_S}{\Phi_{pack}}\right) + 0.85\left(\frac{\Phi_S}{\Phi_{pack}}\right)^2\left(1-\frac{\Phi_S}{\Phi_{pack}}\right)^{-2/3}} \tag{3}$$

$$F_2\left(St_0\right) = \frac{\frac{St_0}{45}+1}{\frac{3St_0}{45}+1} \tag{4}$$

where U_0 represents the Stokes velocity.

Most of the studies of the literature[41] deal with cases where the effect of both inertia of the fluid and that of the particles is negligible ($Re \to 0$, $St_0 \to 0$), so that the sedimentation velocity U_{sed} does not depend either on the Reynolds number or on the Stokes number. In this context, equation (2) reduces to $U_{sed} = U_0\ (1-\Phi_s)\ F_1\left(\frac{\Phi_s}{\Phi_{pack}}\right)$.

As $(\rho_s - \rho_f)(1-\Phi_s) = \rho_s - \rho_m$, the first term $U_0(1-\Phi_s)$ amounts at rewritting the Stokes velocity as $U_{\text{ref}} = \frac{g(\rho_s-\rho_m)d^2}{18\ \mu_f}$ and thus at considering that particle falls in a fluid with a density equivalent to that of the suspension ρ_m, taking into account the effect of the mixture buoyancy. The decreasing function $F_1\left(\frac{\Phi_s}{\Phi_{pack}}\right)$ allows to take into account the effect of the solid concentration of the mixture, thus considering the equivalent fluid viscosity μ_m, so that $U_{sed} = \frac{g(\rho_s-\rho_m)d^2}{18\ \mu_m}$, see

ref.[15,37]. This leads to impose two boundary conditions. For the dilute regime ($\Phi_s \to 0$), equation (2) reduces to $U_{sed} = U_0$, implying that $F_1(0) = 1$ (Figure 2a). For the dense regime ($\Phi_s \to \Phi_{pack}$), $U_{sed} = 0$, implying that $F_1(1) = 0$ (Figure 2a). Far from the packing state, $F_1\left(\frac{\Phi_s}{\Phi_{pack}}\right)$ is described by an exponential law followed by a divergent power law close to the packing state, as commonly described in the literature[41]. In between, the term proportional to $\left(\frac{\Phi_s}{\Phi_{pack}}\right)^2$ allows the asymptotic matching, remaining weak close to the dilute regime while tending towards unity at the packing state (Figure 2a).

In this study, we are interested in cases where the particle inertia can be important ($\frac{\rho_s}{\rho_f} \gg 1$) and can not be neglected. Results expose that equation (2) requires a correction described by a decreasing function $F_2(St_0)$ to take into account the effect of the particle agitation, where $F_2(0) = 1$ respects the Stokes velocity and $F_2(\infty) \to \frac{1}{3}$ reaches a threshold value highlighting a damping effect at high Stokes numbers (Figure 2a).

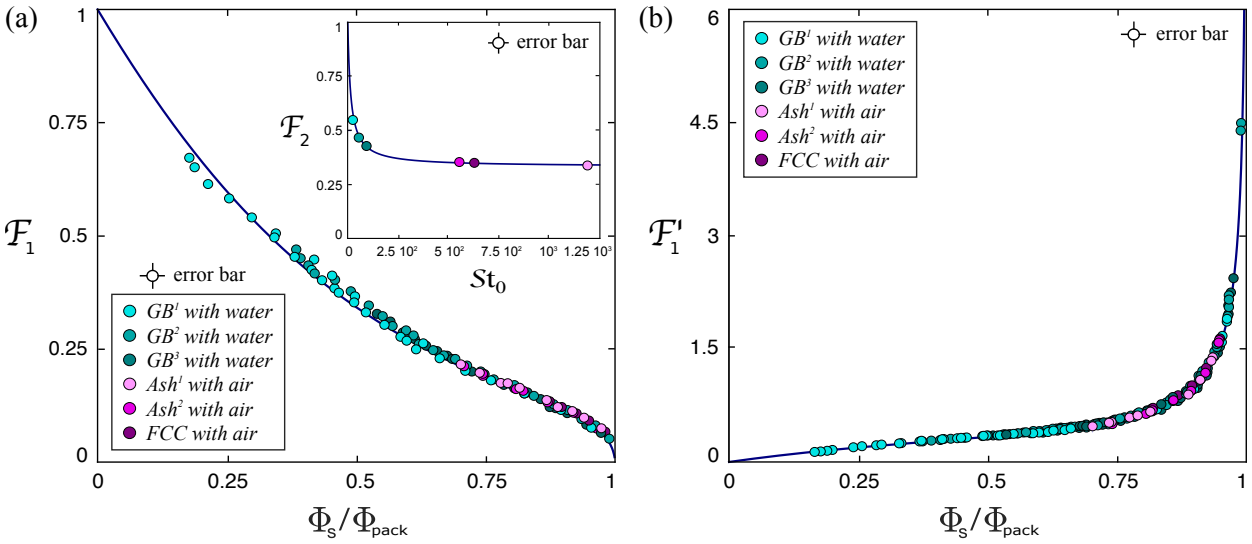

FIG. 2. (a) Experimental measurements of U_{sed} and U_f for the different fluid-particle systems, gathered together on decreasing functions $F_1\left(\frac{\phi_s}{\phi_{pack}}\right)$ and $F_2(St_0)$ of equations (2), (3), (4). (b) Data of U_{agg_0} for identical systems gathered together on the decreasing function $F_1' = \frac{F_1}{\left(\frac{\phi_{pack}}{\phi_s} - 1\right)}$.

From equations (2), (3), (4), U_{sed} appears smaller in static, homogeneous and concentrated suspensions than in a pure fluid. Effects of ρ_m and μ_m tend to reduce its value compared to the theoretical reference velocity U_0. This is however not the case for a cluster of particles that sediments in a pure fluid, around which the streamlines follow the shape of the cloud, reducing the

drag force exerted on it, and thus increasing the particles settling velocity compared to that of an isolated particle[42]. In the case of homogeneous suspensions, streamlines flow around each particle of the mixture, increasing the drag force exerted on it, thus reducing its sedimentation velocity.

Mean aggradation velocities of the basal deposit U_{agg_0}, deduced from measurements of U_{sed} with an accuracy of $\pm 3\%$ (Figure 2b), also gather on a master curve, expressed as :

$$U_{agg_0} = U_0 \left(1 - \Phi_s\right) F_1'\left(\frac{\Phi_s}{\Phi_{pack}}\right) F_2\left(St_0\right) \tag{5}$$

$$F_1'\left(\frac{\Phi_s}{\Phi_{pack}}\right) = \frac{F_1\left(\frac{\Phi_s}{\Phi_{pack}}\right)}{\left(\frac{\Phi_{pack}}{\Phi_s} - 1\right)} \tag{6}$$

Note that for a given fluid-solid system, U_{agg_0} can be easily deduced from the control parameter U_f or the settling velocity of the suspension surface U_{sed} and does not necessary require transparent side-walls and the use of a high speed video camera.

III. SEDIMENTATION OF FLOWING SUSPENSIONS

A. General flow behavior and deposits

As described above, the fully-fluidized suspension is carefully generated in the reservoir where the mixture expansion $\frac{h_s}{h_d}$, fixed in each experiment, allows for controling the mixture concentration $\frac{\Phi_s}{\Phi_{pack}}$ before release. When opening the sliding gate, the fluid-particle suspension travels into a horizontal and impermeable flume where it spreads out until running out of mass (Figure 3).

Gas-solid suspensions were performed by heating both the reservoir, particles and injected air at temperature of 180^oC to get non-cohesive mixtures, while liquid-solid suspensions were made taking the reservoir, particles and injected water at room temperature (around 25^oC). During propagation, the suspension forms a fast-moving and short-lived flow from which we can measure the runout duration T_∞, the traveled distance L_∞, the frontal velocity U_F, the deposit height h_d that reaches its maximum thickness h_{d_∞} at the lock gate, and the deposit slope S.

Gas-solid and liquid-solid suspensions were generated in two specific configurations. In gas-solid experiments, the suspension length and width were of $x_0 = 0.3m$ and $w_0 = 0.15m$. The solid concentration $\frac{\Phi_s}{\Phi_{pack}}$ ranged from 0.65 to 0.95 and varied by either fixing the particle height $h_d = 0.16m$ while increasing the suspension height h_s from 0.16 to $0.25m$; or fixing the suspension height $h_s = 0.25m$ and decreasing the particle height h_d from 0.25 to $0.16m$. In liquid-solid

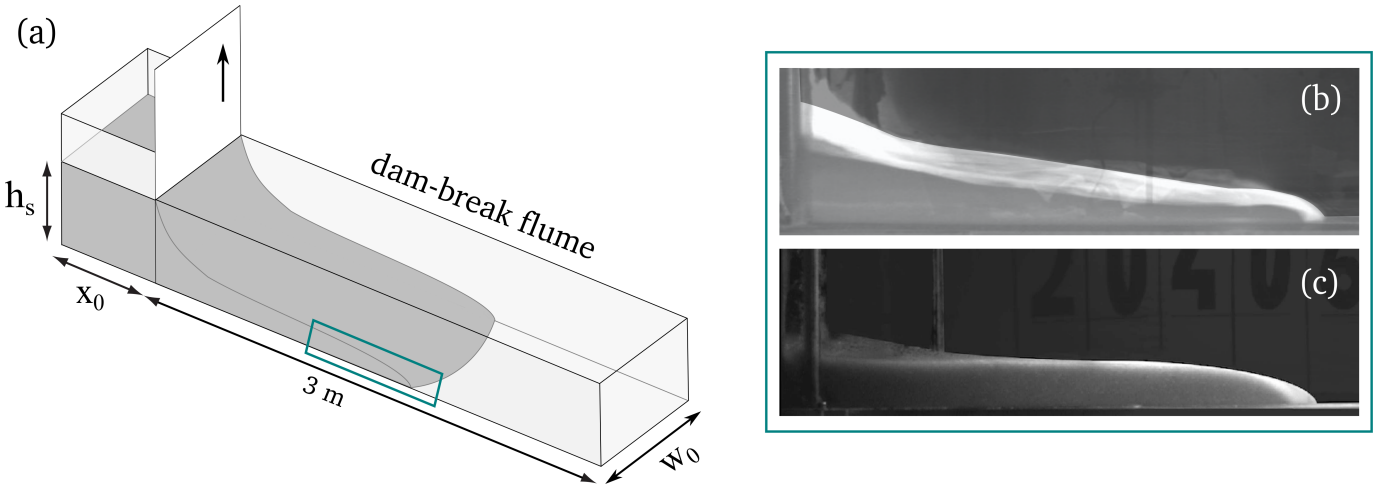

FIG. 3. (a) Scheme of the dam-break flow experiments used for both liquid-solid and gas-solid suspensions. (b) Picture of the frontal region of a gas-solid suspension flowing down the flume. (c) Picture of the frontal region of a liquid-solid suspension during propagation.

experiments, the suspension length and width in the reservoir were respectively of $x_0 = 0.10m$ and $w_0 = 0.30m$. The solid concentration $\frac{\Phi_s}{\Phi_{pack}}$ ranged from 0.70 to 0.95 and varied by fixing the suspension height $h_s = 0.27m$ and decreasing the particle height h_d from 0.27 to $0.19m$. In all experiments, the flume length was taken as $L_f = 3m$. All suspensions behave as classical dam-break flows. Except during both the initial gravitational collapse and the final stopping phase, the suspension front travels at constant velocity $U_{\mathscr{F}}$, ranged from 1 to 2.5 $m.s^{-1}$, that decreases with increasing particle concentration (Figure 4). Flow runouts (duration and distance) both decrease linearly with increasing particle concentration (Figure 5). Normalizing the flow length x by the runout distance L_∞ and the flow time t by the runout duration T_∞ exposes a similar kinematics for all suspensions (Figure 4). As in settling experiments made from static suspensions, the mixture progressively develops a basal deposit overlaid by a homogeneous suspension and an upper fluid layer, whenever this latter is of different nature than the ambiant fluid. Despite the high Reynolds number of the flow, the sedimentation process develops in the Stokes flow regime in which the effects of the fluid inertia are negligible[31]. After the flow has ceased, the particles remain at rest down the flume and form a final deposit while the fluid lies above (liquid-solid mixtures) or mixes with the environnement (gas-solid mixtures). In all cases, the deposit geometry is related to the mixture concentration. The more concentrated the suspensions, the less they flow, the thicker the deposits and the greater the slope. Otherwise, the more dilute the suspensions, the more they flow,

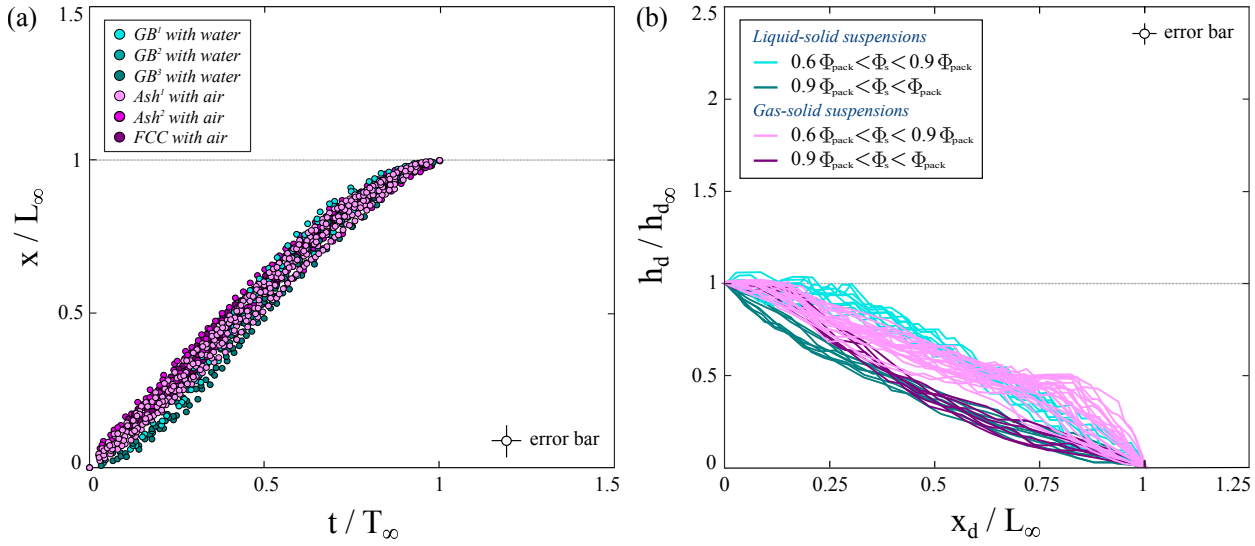

FIG. 4. (a) Flow kinematics measured from fluid-particle systems : frontal position x normalized by the runout distance L_∞ as a function of time t normalized by the runout duration T_∞. (b) Flow deposits measured from fluid-particle systems : deposit height h_d normalized by the runout thickness at the lock gate h_{d_∞} as a function of the deposit length x_d normalized by the runout distance L_∞.

the thinner the deposits and the more gentle the slope (Figure 4). By normalizing the deposit height h_d by the maximum thickness h_{d_∞} and the deposit length x_d by the runout distance L_∞, two types of profiles can be distinguished. For both liquid-solid and gas-solid flows, highly concentrated suspensions ($0.9 \leq \frac{\Phi_s}{\Phi_{pack}} \leq 1$) form a triangular deposit with a constant slope, represented by dark colors in Figure 4. In those cases, sedimentation is initiated just after the gravitational collapse when the flow is being established, at the beginning of the longest phase of transport. Conversely, slightly loaded liquid-solid and gas-solid suspensions ($0.65 \leq \frac{\Phi_s}{\Phi_{pack}} \leq 0.9$) form a trapezoidal deposit with a constant slope preceded by a plateau, represented by light colors in Figure 4. The presence of this plateau should mean that the sedimentation may start after a critical time t_c at a critical length x_c, corresponding to the phase of gravitational collapse, thus depending on the initial conditions and the reservoir geometry. Then, the deposit height aggrades upwards at a velocity U_{agg}, roughly constant with time and space during the flow[16] that spreads at constant velocity $U_{\mathscr{F}} \propto \sqrt{\left(\frac{\rho_s-\rho_f}{\rho_s}\right) 2gh_s}$ (Figure 6), thus forming a deposit of constant slope S[31]. This implies that simple measurements of deposit slope, frontal velocity, and flow runout are sufficient to infer the aggradation velocity from flowing suspensions.

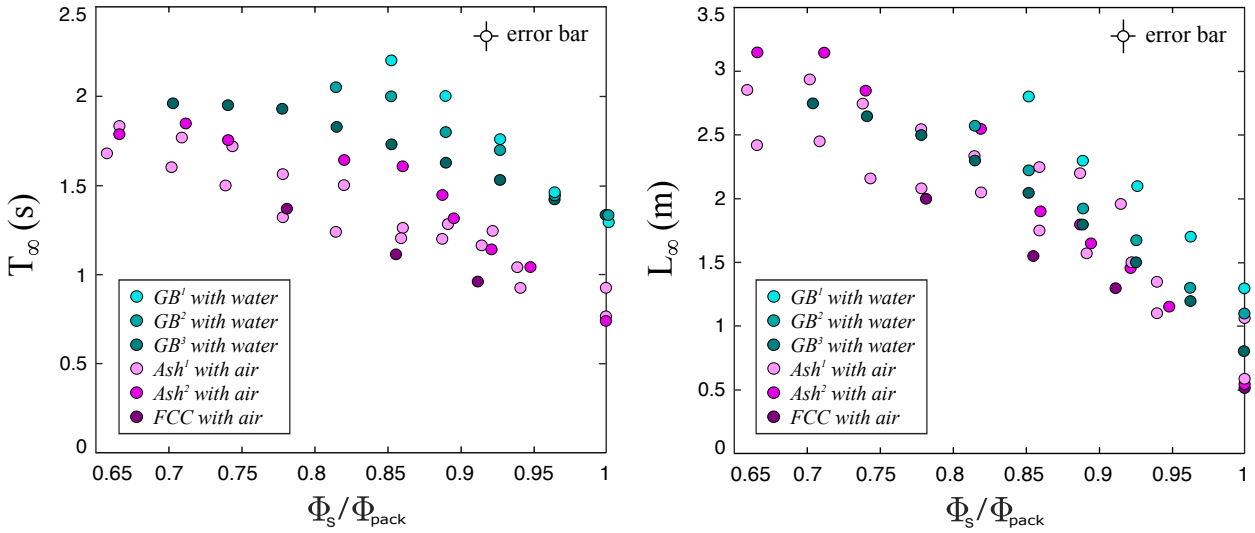

FIG. 5. (a) Runout duration T_∞ and (b) runout length L_∞ as a function of the mixture concentration $\frac{\Phi_s}{\Phi_{pack}}$ measured from fluid-particle systems.

B. Presentation of the physical model

In the aim of describing results obtained with different fluid-particle systems, we propose a physical model able to describe the general features of the flows (kinematics, sedimentation) and their deposits, based on three principal assumptions, summarized as follow :

A1 – The mixture is made of three homogeneous layers :

· a fluid-particle suspension, of solid concentration Φ_s constant in time and space, that progressively defluidizes and sediments during travel ;

· a basal deposit, of solid concentration Φ_{pack} constant in time and space, that progressively thickens during propagation ;

· an upper pure fluid layer ($\Phi_s = 0$), that continuously thickens (liquid) or dissipates (gas) during the flow, at a velocity $U_f = U_{sed}$ that remains constant in time and space.

A2 – During propagation, particles sediment from the suspension at a constant velocity U_{sed}, over a distance $L_{sed} = L_\infty - x_c$ and during a period $T_{sed} = T_\infty - \frac{x_c}{U_{\mathscr{F}}}$, to form a deposit that thickens at a constant velocity U_{agg}. As in static suspensions, deposition develops in the Stokes flow regime whereas the dam-break flow is inertial.

A3 – During the sedimentation phase, the front of the flow travels at a constant velocity $U_{\mathscr{F}}$ that scales as $\sqrt{\left(\frac{\rho_s - \rho_f}{\rho_s}\right) 2gh_s}$.

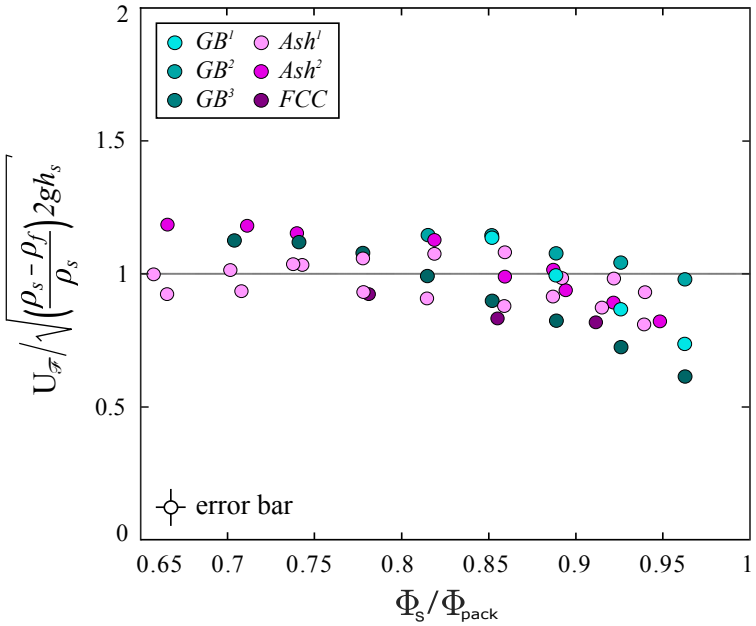

FIG. 6. Non dimensional flow front velocity $U_{\mathscr{F}}$ measured during the constant-velocity phase normalized by $\sqrt{\left(\frac{\rho_s-\rho_f}{\rho_s}\right)2gh_s}$ as a function of $\frac{\Phi_s}{\Phi_{pack}}$.

Assumptions **A2** and **A3** lead to express the deposit slope S as follow :

$$h_d(x,t) = \int_{T_0=\frac{(x-x_c)}{U_{\mathscr{F}}}}^{T_\infty} U_{agg}\ \ dt = U_{agg}\left[T_\infty - \frac{(x-x_c)}{U_{\mathscr{F}}}\right],$$

$$S = \frac{\partial h_d(x,t)}{\partial x} = -\frac{U_{agg}}{U_{\mathscr{F}}}. \tag{7}$$

From that follows the expression of the sedimentation duration T_{sed} and sedimentation length L_{sed}, by assuming that $U_{\mathscr{F}} = \frac{L_{sed}}{T_{sed}}$:

$$T_{sed} = \frac{h_{d_\infty}}{U_{agg}}, \tag{8}$$

$$L_{sed} = \frac{h_{d_\infty}}{S}. \tag{9}$$

As a result, we are able to model the general features of the suspensions when their flow is fully established and behaves in a simple way : with a constant frontal velocity $U_{\mathscr{F}}$, a constant aggradation velocity U_{agg}, and a constant deposit slope S; while the critical time and length, t_c and x_c, requires the model of the gravitational collapse which depends on initial conditions, such as :

$$\begin{cases} t_c \propto a\sqrt{\frac{h_s}{g}}, \\ x_c \propto \frac{a}{S}\sqrt{\frac{h_s}{g}}U_{agg}. \end{cases} \tag{10}$$

where h_s represents the initial thickness of the suspension, and $a = \frac{h_s}{x_0}$: its aspect ratio.

C. Sedimentation of spreading suspensions

From the physical model, the aggradation velocity of flowing suspensions, $U_{agg} = SU_{\mathscr{F}}$, can thus be simply deduced from experiments by measuring the flow velocity and deposit slope at a given concentration Φ_s. To assess the relevance of the proposed physical model in the description of the first-order feature of sedimenting dam-break suspension flows, we first measure the evolution of the deposit thickness with time in flows of moderately concentrated suspensions ($\frac{\Phi_s}{\Phi_{pack}} = 0.855$) for both a liquid-solid and a gas-solid suspension in aid of a high-speed video camera calibrated at 1200 frames per second (Figure 7a) at the vicinity of the sliding gate ($x = 0.30 - 0.60m$), where the deposit height is maximum. Once the particles deposition is initiated (from $t \geq t_c$), measurements expose an aggradation velocity V_{agg} that can reasonably assumed to be constant (Figure 7a). Then, comparing predictions of mean aggradation velocities U_{agg} with measurements V_{agg} made on proximal areas (*i.e.* over the first 0.60m of the channel) during propagation, exposes a satisfying correlation of results gathered along the line $U_{agg} = V_{agg}$ (Figure 7b). These results highlight that the flow velocity and deposit slope, that can be easily measured in natural flows, are sufficient to predict the first-order value of the aggradation velocity in fully established flows traveling in distal (almost flat) areas. Now, plotting the ratio of the aggradation velocity measured in static suspensions U_{agg_0} and that predicted in flowing suspensions U_{agg} exposes that the ratio remains surprisingly close to unity for both gas-solid and liquid-solid suspensions involving small and light particles, with $d \leq 300\mu m$ and $\rho_s \leq 2500kg.m^{-3}$, and does not depend on the mixture concentration $\frac{\Phi_s}{\Phi_{pack}}$ (Figure 8a). Otherwise for liquid-solid suspensions, made with coarse and dense particles, the aggradation velocity in flowing suspensions becomes significantly reduced compared to that measured in static mixtures. Figure 8b exposes this ratio as a function of the Reynolds number, based on the particle diameter d and the mean flow velocity $U = \frac{L_\infty}{T_\infty}$, which compares the fluid inertia to viscous stress at the scale of the particles. We observe that the aggradation velocity of flowing suspensions is significantly affected by the mixture agitation from a threshold value of $Re \geq 250$ and tends to significantly decrease in comparison with lower Re suspension flows. This important result means that when $Re \leq 250$, the suspension flow can be described as a low-viscosity quasi-parallel flow[31] with no significant vertical velocity fluctuations capable of altering the particles motion. As particles settle vertically throughout the flow during propagation, the description of the sedimentation process can be decoupled from that of the flow and remains quasi-identical to that studied in detail in static suspensions. Above the

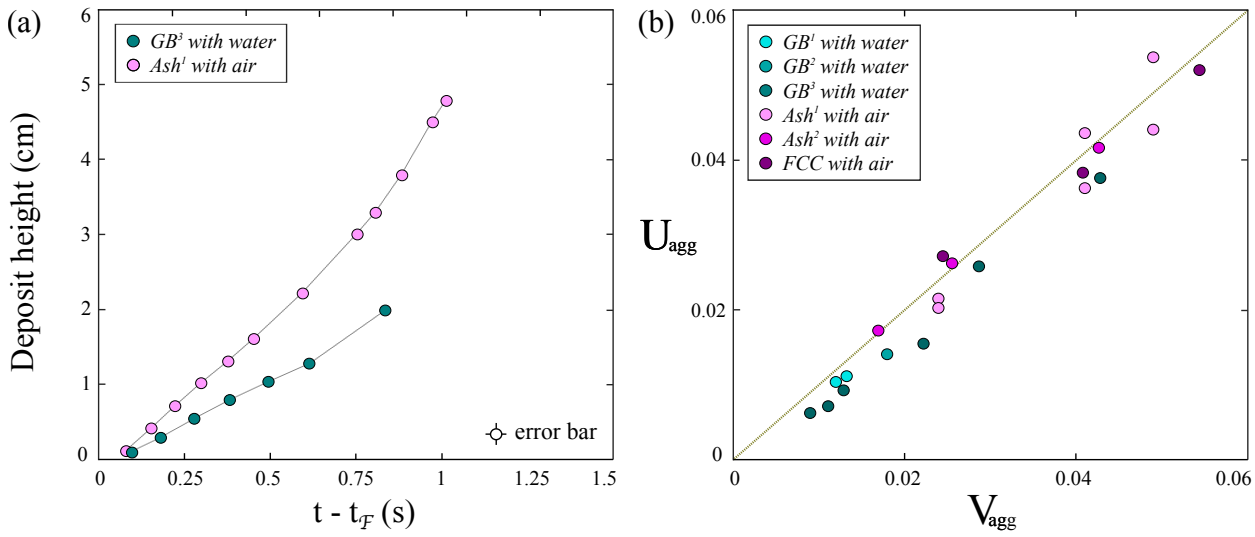

FIG. 7. (a) Deposit height h_d measured as a function of the time relatively to the passage of the flow front $t - t_{\mathscr{F}}$ in aid of a high-speed video camera fixed at 1200 Hz for both a liquid-solid and a gas-solid suspension characterized by a particle concentration of $\frac{\Phi_s}{\Phi_{pack}} = 0.855$. (b) Prediction of particles aggradation velocities U_{agg} against measurements of particles aggradation velocities V_{agg} in flowing suspensions for both liquid-solid and gas-solid mixtures at different particle concentrations $\frac{\Phi_s}{\Phi_{pack}}$.

threshold value of Re, the fluid inertia becomes important enough to develop fluctuating eddies, at the scale of the particle, which significantly disturb and delay their sedimentation. In that case, the particle deposition can not be decoupled from the global flow. A detailed study is required to understand how the mean velocity gradient and fluctuations can impact the sedimentation velocity.

This simplified model highlights that we are able to describe the final stage of particulate suspensions, far from the source, when the flow is dominated by sedimentation and that large particles have been deposited down volcanic flanks or valleys at the head of the watershed. In this situation, the flow has henceforth a narrow distribution in particle sizes or density, which does not allow segregation in size or in density, and becomes established enough to travel at constant speed down valleys made with gentle slopes or near coastal areas. Then, if the solid concentration of the mixture remains approximately constant in time and space (*i.e.* if sedimentation velocity is quite similar to that of the fluid expel), we can provide a reliable order of magnitude of the sedimentation rate using physical parameters that can be easily measured on the field or from video footages, as the deposit slope and the mean flow velocity during this final phase of transport[1–3]. Furthermore, this allows us to infer in return the physical properties of natural mixtures, such as

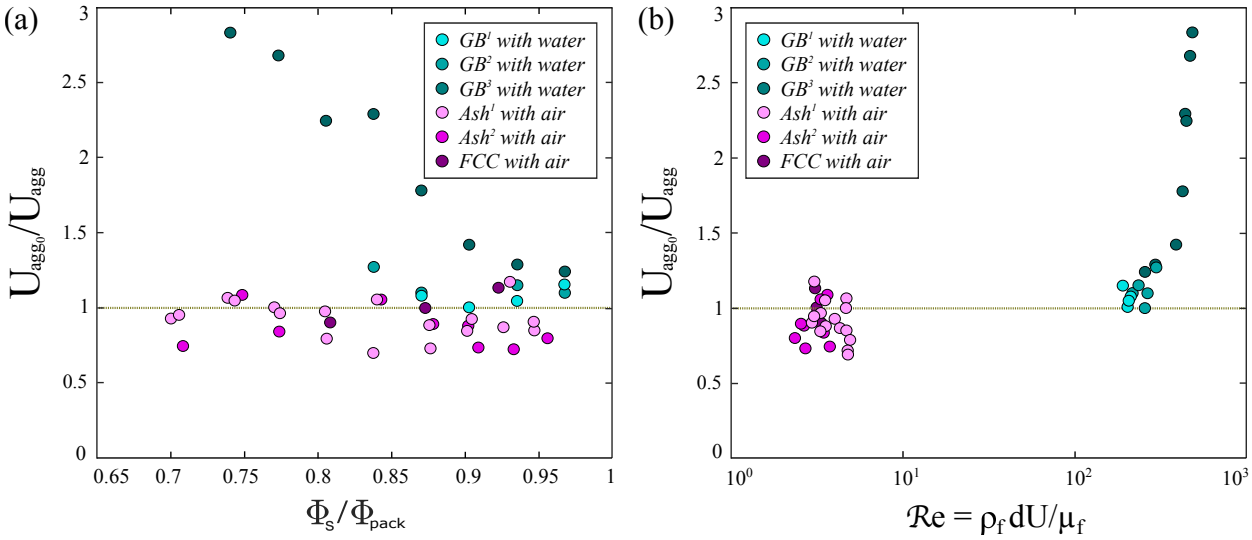

FIG. 8. (a) Non dimensional ratio of deposit aggradation velocities measured in static suspensions U_{agg_0} and predicted in flowing suspensions U_{agg} as a function of $\frac{\Phi_s}{\Phi_{pack}}$. (b) Non dimensional ratio $\frac{U_{agg_0}}{U_{agg}}$ as a function of the Reynolds number Re that compares the fluid inertia to the viscous stress at the scale of the particles.

the volume expansion $\frac{\Phi_{pack}}{\Phi_s}$ as well as the solid concentration Φ_s (from the measurement of the deposit compacity Φ_{pack}) during their final phase of transport. The present model of sedimentation can be then implemented in large-scale simulations where the flow is propagating down a real topography using a digital field model in the aim of producing probabilistic hazard mapping of such extreme events[43]. This model may be applied to pyroclastic flows, lahars, or non-colloidal mud flows, mostly made with non-cohesive hot volcanic ash, tephras, or silty-sandy particles, suspended into a fluid, and that travel long distances down roughly flat valleys.

IV. CONCLUSION

In this paper, we propose a general model of the sedimentation velocity in homogeneous suspensions in which deposition, that involve flows at the scale of the particle, is dominated by viscous stresses (*i.e.* in the Stokes flow regime where the fluid inertia is negligible). This law describes the particle settling as that of an isolated particle falling into a mixture of equivalent properties, including the effect of the mixture density ρ_m (described by the function 1-Φ_s) that affects the buoyant force acting on each particle, and the effect of the mixture viscosity μ_m, that includes the effect of the solid concentration $\frac{\Phi_s}{\Phi_{pack}}$ and that of the particles inertia St_0 (respectively described

by functions F_1 and F_2) which affects the drag force acting on each particle. This law is general in that it applies to all types of non cohesive particles and fluids, gas or liquid, whatever the density ratio between the particles and fluid. Unlike to sedimentation processes, dam-break suspension flows develop at high Reynolds numbers and can become agitated. Except during both the initial and final short-lived phases, flows travel at constant velocity, proportional to $\sqrt{\left(\frac{\rho_s-\rho_f}{\rho_s}\right)2gh_s}$, and progressively sediment from the base at a velocity U_{agg}, constant in time and space, to form a triangular or trapezoidal deposit. Their duration is governed by the sedimentation time, so that −if $U_{\mathscr{F}}$ and U_{agg} are constant− the deposit slope S is constant and corresponds to the ratio of the two characteristic velocities $S = \frac{U_{agg}}{U_{\mathscr{F}}}$. As these physical properties ($U_{\mathscr{F}}$, S) can be simply measured in laboratory experiments or in natural flows, U_{agg} can be predicted in the flows. Preliminary results allow us to compare predictions of U_{agg} with measurements made from static suspensions U_{agg_0} at given concentrations Φ_s. We observed that, as long as the Reynolds number *Re* (based on the flow velocity, the fluid properties, and the particles size) is smaller than a few hundred, particles sediment at the same velocity in flows as in static suspensions. Otherwise, when *Re* becomes greater than several hundred, the sedimentation velocity sharply decreases in flows and requires additional studies to analyze these aspects related to the mixture agitation. These important results make possible the description of the sedimentation dynamics, as well as the mixture rheology, in natural flows (such as pyroclastic flows, lahars, non-colloidal mud flows), difficult to observe, from video footages and measurable parameters of the final deposits.

ACKNOWLEDGMENTS

This study was supported by the Region Centre-Val de Loire through the Contribution of 'Academic Initiative': RHEFLEXES/2019-00134935.

DATA AVAILABILITY STATEMENT

The data supporting the findings of this study are available in this manuscript.

REFERENCES

[1]R. P. Hoblitt, *Observations of the eruptions of July 22 and August 7, 1980, at Mount St. Helens, Washington*, Vol. 1335 (US Government Printing Office, 1986).

[2]A. H. Levine and S. W. Kieffer, "Hydraulics of the august 7, 1980, pyroclastic flow at mount st. helens, washington," Geology **19**, 1121–1124 (1991).

[3]S. Loughlin, E. Calder, A. Clarke, P. Cole, R. Luckett, M. Mangan, D. Pyle, R. Sparks, B. Voight, and R. Watts, "Pyroclastic flows and surges generated by the 25 june 1997 dome collapse, soufrière hills volcano, montserrat," Geological Society, London, Memoirs **21**, 191–209 (2002).

[4]R. S. J. Sparks, "Grain size variations in ignimbrites and implications for the transport of pyroclastic flows," Sedimentology **23**, 147–188 (1976).

[5]T. H. Druitt and B. P. Kokelaar, "The eruption of soufrière hills volcano, montserrat, from 1995 to 1999," (Geological Society of London, 2002).

[6]M. J. Branney and B. P. Kokelaar, "Pyroclastic density currents and the sedimentation of ignimbrites," (Geological Society of London, 2002).

[7]J. W. Vallance and R. M. Iverson, "Lahars and their deposits," in *The encyclopedia of volcanoes* (Elsevier, 2015) pp. 649–664.

[8]J.-C. Thouret, S. Antoine, C. Magill, and C. Ollier, "Lahars and debris flows: Characteristics and impacts," Earth-Science Reviews **201**, 103003 (2020).

[9]E. Lajeunesse, J. Monnier, and G. Homsy, "Granular slumping on a horizontal surface," Physics of fluids **17** (2005).

[10]G. Lube, H. E. Huppert, R. S. J. Sparks, and A. Freundt, "Collapses of two-dimensional granular columns," Physical Review E—Statistical, Nonlinear, and Soft Matter Physics **72**, 041301 (2005).

[11]L. Girolami, T. Druitt, O. Roche, and Z. Khrabrykh, "Propagation and hindered settling of laboratory ash flows," Journal of Geophysical Research: Solid Earth **113** (2008).

[12]A. Freundt, "Entrance of hot pyroclastic flows into the sea: experimental observations," Bulletin of Volcanology **65**, 144–164 (2003).

[13]T. C. Pierson, A. S. Daag, P. Delos Reyes, M. T. M. Regalado, R. U. Solidum, and B. S. Tubianosa, "Flow and deposition of posteruption hot lahars on the east side of mount pinatubo, july–october 1991," Fire and Mud: eruptions and lahars of Mount Pinatubo, Philippines , 921–950 (1996).

[14]C. Wilson, "The role of fluidization in the emplacement of pyroclastic claws: An experimental approach," Journal of Volcanology and geothermal Research **8**, 231–249 (1980).

[15]A. Amin, L. Girolami, and F. Risso, "On the fluidization/sedimentation velocity of a homogeneous suspension in a low-inertia fluid," Powder Technology **391**, 1–10 (2021).

[16]L. Girolami, O. Roche, T. H. Druitt, and T. Corpetti, "Particle velocity fields and depositional processes in laboratory ash flows, with implications for the sedimentation of dense pyroclastic flows," Bulletin of Volcanology **72**, 747–759 (2010).

[17]O. Roche, "Depositional processes and gas pore pressure in pyroclastic flows: an experimental perspective," Bulletin of Volcanology **74**, 1807–1820 (2012).

[18]J. Dufek, "The fluid mechanics of pyroclastic density currents," Annual Review of Fluid Mechanics **48**, 459–485 (2016).

[19]G. A. Valentine, "Initiation of dilute and concentrated pyroclastic currents from collapsing mixtures and origin of their proximal deposits," Bulletin of Volcanology **82**, 20 (2020).

[20]B. J. Andrews and M. Manga, "Experimental study of turbulence, sedimentation, and coignimbrite mass partitioning in dilute pyroclastic density currents," Journal of Volcanology and Geothermal Research **225**, 30–44 (2012).

[21]T. E. Ongaro, S. Orsucci, and F. Cornolti, "A fast, calibrated model for pyroclastic density currents kinematics and hazard," Journal of Volcanology and Geothermal Research **327**, 257–272 (2016).

[22]E. Brosch and G. Lube, "Spatiotemporal sediment transport and deposition processes in experimental dilute pyroclastic density currents," Journal of Volcanology and Geothermal Research **401**, 106946 (2020).

[23]E. Doyle, A. Hogg, H. Mader, and R. Sparks, "Modeling dense pyroclastic basal flows from collapsing columns," Geophysical Research Letters **35** (2008).

[24]H. A. Shimizu, T. Koyaguchi, and Y. J. Suzuki, "The run-out distance of large-scale pyroclastic density currents: a two-layer depth-averaged model," Journal of Volcanology and Geothermal Research **381**, 168–184 (2019).

[25]H. A. Shimizu, T. Koyaguchi, Y. J. Suzuki, E. Brosch, G. Lube, and M. Cerminara, "Validation of a two-layer depth-averaged model by comparison with an experimental dilute stratified pyroclastic density current," Bulletin of Volcanology **83**, 73 (2021).

[26]S. P. Pudasaini, "A general two-phase debris flow model," Journal of Geophysical Research: Earth Surface **117** (2012).

[27]E. Calder, R. Sparks, and M. Gardeweg, "Erosion, transport and segregation of pumice and lithic clasts in pyroclastic flows inferred from ignimbrite at lascar volcano, chile," Journal of Volcanology and Geothermal Research **104**, 201–235 (2000).

[28]F. Lavigne and J.-C. Thouret, "Sediment transportation and deposition by rain-triggered lahars at merapi volcano, central java, indonesia," Geomorphology **49**, 45–69 (2003).

[29]J. C. Phillips, A. J. Hogg, R. R. Kerswell, and N. H. Thomas, "Enhanced mobility of granular mixtures of fine and coarse particles," Earth and Planetary Science Letters **246**, 466–480 (2006).

[30]J. Gray and B. Kokelaar, "Large particle segregation, transport and accumulation in granular free-surface flows," Journal of Fluid Mechanics **652**, 105–137 (2010).

[31]L. Girolami and F. Risso, "Physical modeling of the dam-break flow of sedimenting suspensions," Physical Review Fluids **5**, 084306 (2020).

[32]L. Rousseau, L. Girolami, and F. Risso, "Propagation of concentration waves in liquid-solid fluidized beds," Physical Review Fluids **In prep.** (2024).

[33]P. Lettieri, J. Yates, and D. Newton, "The influence of interparticle forces on the fluidization behaviour of some industrial materials at high temperature," Powder Technology **110**, 117–127 (2000).

[34]T. H. Druitt, G. Avard, G. Bruni, P. Lettieri, and F. Maez, "Gas retention in fine-grained pyroclastic flow materials at high temperatures," Bulletin of Volcanology **69**, 881–901 (2007).

[35]I. Eames and M. Gilbertson, "Aerated granular flow over a horizontal rigid surface," Journal of Fluid Mechanics **424**, 169–195 (2000).

[36]L. Girolami, *Dynamique et sédimentation des écoulements pyroclastiques reproduits en laboratoire*, Ph.D. thesis, Université de Clermont II (2008).

[37]L. Girolami and F. Risso, "Sedimentation of gas-fluidized particles with random shape and size," Physical Review Fluids **4**, 074301 (2019).

[38]J. F. Richardson and W. N. Zaki, "The sedimentation of a suspension of uniform spheres under conditions of viscous flow," Chemical Engineering Science **3**, 65–73 (1954).

[39]J. F. Richardson and W. N. Z. P. D, "Sedimentation and fluidisation: Part I," Trans. Inst. Chem. Eng. **32**, S82–S100 (1954).

[40]A. R. Abrahamsen and D. Geldart, "Behaviour of gas-fluidized beds of fine powders part I. Homogeneous expansion," Powder Technology **26**, 35–46 (1980).

[41]É. Guazzelli and O. Pouliquen, "Rheology of dense granular suspensions," Journal of Fluid Mechanics **852**, P1 (2018).

[42]B. Metzger, M. Nicolas, and É. Guazzelli, "Falling clouds of particles in viscous fluids," Journal of Fluid Mechanics **580**, 283–301 (2007).

[43]M. de'Michieli Vitturi, A. Costa, M. A. Di Vito, L. Sandri, and D. M. Doronzo, "Lahar events in the last 2000 years from vesuvius eruptions–part 2: Formulation and validation of a computational model based on a shallow layer approach," Solid Earth **15**, 437–458 (2024).